

PACS numbers: 42.81.Bm; 42.81.Cn; 42.81.Dp; 78.60.Lc
DOI: 10.1070/QE2012v042n09ABEH014894

Optical properties of bismuth-doped silica fibres in the temperature range 300–1500 K

D.A. Dvoretskii, I.A. Bufetov, V.V. Vel'miskin, A.S. Zlenko, V.F. Khopin, S.L. Semjonov, A.N. Gur'yanov, L.K. Denisov, E.M. Dianov

Abstract. **The visible and near-IR absorption and luminescence bands of bismuth-doped silica and germanosilicate fibres have been measured for the first time as a function of temperature. The temperature-dependent IR luminescence lifetime of a bismuth-related active centre associated with silicon in the germanosilicate fibre has been determined. The Bi^{3+} profile across the silica fibre preform is shown to differ markedly from the distribution of IR-emitting bismuth centres associated with silicon. The present results strongly suggest that the IR-emitting bismuth centre comprises a low-valence bismuth ion and an oxygen-deficient glass network defect.**

Keywords: *bismuth, bismuth-doped optical fibre, temperature dependence of optical absorption.*

1. Introduction

Bismuth-doped silica fibres are broadband optical gain media [1]. Their optical gain band depends on the composition of their core, which typically consists of bismuth-doped aluminosilicate, germanosilicate, phosphosilicate, phosphogermanosilicate or pure silica (v-SiO_2) glass. Such fibres currently ensure optical amplification and lasing in the range of about 1.15 to 1.55 μm. The efficiency of Bi-doped fibre lasers at a number of wavelengths in this range reaches 50%, and their output power in single-mode cw operation is 20 W [2]. A bismuth-doped germanosilicate fibre has recently been demonstrated to offer a 25-dB gain in a 40-nm-wide band with a centre wavelength of 1440 nm at a pump power as low as 65 mW [3]. All this suggests that bismuth-doped fibres have considerable potential for use as active media of amplifiers and lasers operating in new frequency ranges in continuous mode or ultrashort pulse generation mode [4].

D.A. Dvoretskii Fiber Optics Research Center, Russian Academy of Sciences, ul. Vavilova 38, 119333 Moscow, Russia; Bauman Moscow State Technical University, Vtoraya Baumanskaya ul. 5, 105005 Moscow, Russia;
I.A. Bufetov, V.V. Vel'miskin, A.S. Zlenko, S.L. Semjonov, E.M. Dianov Fiber Optics Research Center, Russian Academy of Sciences, ul. Vavilova 38, 119333 Moscow, Russia; e-mail: iabuf@fo.gpi.ru;
V.F. Khopin, A.N. Gur'yanov G.G. Devyatykh Institute of Chemistry of High-Purity Substances, Russian Academy of Sciences, ul. Tropinina 49, 603950 Nizhnii Novgorod, Russia;
L.K. Denisov Bauman Moscow State Technical University, Vtoraya Baumanskaya ul. 5, 105005 Moscow, Russia

Received 24 April 2012
Kvantovaya Elektronika **42** (9) 762–769 (2012)
Translated by O.M. Tsarev

Unfortunately, none of the models proposed to date for IR-emitting Bi-related active centres (BACs) in bismuth-doped fibres (or glasses) has been supported by direct experimental evidence [5, 6]. This circumstance is a serious obstacle to further improvements in the performance of the new type of gain medium.

The luminescence properties of bismuth-doped fibres of various compositions have recently been the subject of detailed studies. It has been shown that BACs with the simplest energy level diagrams are present in bismuth-doped fibres made from pure silica glass (SBi fibres), as well as from germanate (GBi fibres) and germanosilicate (GSBi fibres) glasses [7]. The energy level diagram in aluminosilicate and phosphosilicate glasses is considerably more complex.

The study of the temperature effect on the properties of BACs is one of the approaches capable of shedding light on their physical nature. Such experiments were carried out by Bulatov et al. [8] for aluminosilicate fibres at several temperatures (77, 300, 600 and 1000 K). However, their results are difficult to adequately interpret because there is a limited set of experimental data and because the BACs in aluminosilicate glasses have a complex energy level diagram (in comparison with, e.g., SBi fibres).

In studies concerned with laser damage in optical fibres (so-called fibre fuse effect), the optical loss in fibres (free of IR-emitting centres) was measured up to about the glass transition temperature T_g of silica glass [9–11]. The results indicate that, below $T \approx 1000\,^{\circ}C$, the optical loss in silica fibres does not exceed ~10 dB km^{-1}. At the same time, starting near 1050 °C [9] (or 1150 °C [11]) the loss increases sharply, reaching 2000 dB km^{-1} at a 50 °C higher temperature. Thus, at temperatures below 1100 °C and optical losses above several dB km^{-1}, silica fibres can be used to deliver light to a fibre sample in a high-temperature zone without significant distortions of measurement results.*

The loss at absorption peaks of IR-emitting bismuth centres in fibre ranges from 10^3 to 10^6 dB km^{-1} [7], suggesting that the absorption in bismuth-doped fibres should be measured in the spectral range of these peaks. It seems likely that, for the temperature dependences of the properties of BACs to show up more clearly, measurements should be extended to higher temperatures (in the case of glass fibres, T_g is a characteristic temperature in this range).

* More detailed experimental data on the optical loss in bismuth-free fibres of various compositions are currently in preparation for publication.

In this paper, we report the optical loss and luminescence spectra of SBi and GSBi fibres between room temperature and 1200 °C.

2. Samples and measurement conditions

We studied Bi-doped silica fibres containing no other dopants (two samples) and a silica fibre codoped with bismuth and germanium (Table 1). The fibres were produced by different processes: the powder-in-tube (PIT) method [12] was used to prepare the preform of fibre 1, whereas fibre 2 was produced by FCVD (a variant of MCVD) [13]. The guidance properties of the core in fibre 1 were due to a fluorine-doped reflective (depressed) silica cladding, and those of the core in fibre 2 were due to a microstructured, air-filled holey cladding. Fibre 3 was fabricated by the MCVD process, and its core, based on v-SiO_2, contained 5 mol % germanium oxide, which ensured an appropriate refractive index profile in the fibre. The outer diameter of all the fibres was 125 μm (without the polymer coating). Note that the three types of fibres were shown earlier to lase in the spectral region from about 1400 to 1500 nm [2, 12, 13].

The fibre core composition was determined using a JSM 5910LV scanning electron microscope equipped with an X-ray microanalysis system (Oxford Instruments). In all the samples, the bismuth content was below the detection limit (under 0.02 at %), so it is not specified in Table 1.

Table 1. Designations, core compositions and fabrication techniques of the fibres.

Fibre	Core composition (%)	Preform fabrication technique	Ref.
SBi-P (1)	$100SiO_2-Bi_2O_3$	PIT	[12]
SBi-H (2)	$100SiO_2-Bi_2O_3$	FCVD	[13]
GSBi (3)	$95SiO_2-5GeO_2-Bi_2O_3$	MCVD	[2, 3]

To heat the fibres, we used a tubular electric furnace having a cylindrical working space 100 cm in length and 2 cm in diameter. The working space was not sealed and was always filled with ambient air. The isothermal zone, with a temperature field uniform to within ±3 °C, was 40 cm long. The furnace temperature was varied from 25 to 1200 °C. The average heating rate in the isothermal zone was 25 °C min^{-1} at temperatures from 30 to 700 °C and gradually decreased to 10 °C min^{-1} between 700 and 1200 °C. The fibres were first heated at these rates from room temperature (RT) to 1200 or 1000 °C (in different experiments) and then slowly cooled (in several hours) to their initial temperature. The temperature was monitored with an accuracy of ±0.5 °C. Prior to measurements, a stripped fibre was placed along the axis of the isothermal zone in air. Its length was no greater than that of the isothermal zone. The fibre ends were fusion spliced to pieces of passive silica fibres for coupling and decoupling a test beam.

Optical loss and luminescence spectra were measured during heating of the fibres and after cooling to RT. For this purpose, we used an HP 70950B optical spectrum analyser in the range 750–1700 nm and an Ocean Optics S2000 spectrometer between 350 and 850 nm. The optical loss in the fibres was determined by a standard cut-back technique (comparison of the spectral powers transmitted by a short piece and long length of the fibre). The test fibre length was limited by the length of the isothermal zone, which prevented us from measuring the optical loss in the spectral range 850–1700 nm, where it was too low.

The luminescence spectra of the bismuth-doped fibres were taken at various temperatures between the excitation wavelength (457 or 808 nm) and 1700 nm. Excitation was provided by a frequency-doubled neodymium laser at 914 nm (second harmonic power, 100 mW) or a fibre-pigtailed single-mode semiconductor laser diode (wavelength, 808 nm; output power, 100 mW). To rule out the influence of luminescence reabsorption in the fibre core, the luminescence spectrum was measured through the lateral surface of the fibre in a configuration similar to that described by Mattsson [14].

To measure the temperature-dependent luminescence decay time of the IR-emitting bismuth centres in the spectral range 1300–1500 nm, an InGaAs photodiode with a response time of 3 μs was used as a detector. The luminescence was excited by 10-μs laser diode pulses at 808 nm. The signal was recorded by a digital oscilloscope (LeCroy Wavepro 7100).

3. Measurement results

Figure 1 shows the optical loss spectra of the fibres in the visible and near-IR spectral regions at RT. The optical loss spectra of the SBi-P and SBi-H fibres are similar in shape and consist of composite bands peaking at 420, 820 and 1400 nm on top of a background loss which monotonically increases by about two orders of magnitude between 1600 and 400 nm. The GSBi fibre has a lower average level of losses and a differ-

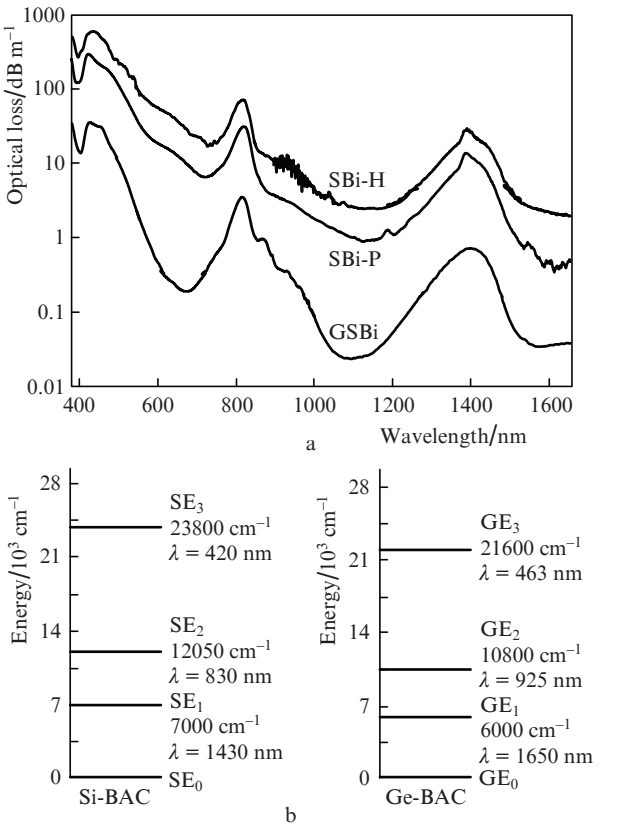

Figure 1. (a) Optical loss spectra of the germanosilicate fibre GSBi and the bismuth-doped silica fibres SBi-P and SBi-H. (b) Energy level diagrams of the Si-BAC and Ge-BAC.

ent shape of the absorption bands at 420 and 1400 nm. In contrast to that in the SBi-P and SBi-H fibres, the 820-nm absorption has several weak, poorly discernible features on its long-wavelength side, between 870 and about 1000 nm. As shown earlier [7], the features at 460 and 940 nm, present in the spectrum of the GSBi fibre (Fig. 1) as components of composite absorption bands, are due to BACs associated with germanium atoms (Ge-BACs). These centres were observed to luminesce near 950 and 1650 nm.

The absorptions near 420, 820 and 1400 nm in the GSBi, SBi-P and SBi-H fibres are due to other BACs, associated with silicon (Si-BACs), which luminesce near 830 and 1400 nm [7, 12]. It is worth noting that the 1400-nm absorption peaks of the Si-BACs in the SBi-H and SBi-P fibres overlap with the 1380-nm absorption bands of OH groups. The positions of the above-mentioned absorption and luminescence lines correspond to transitions between the four lowest energy levels of the Si-BAC and Ge-BAC, whose energy level diagrams are presented in Fig. 1b [7]. In our measurements, particular attention was paid to the variations of the absorption and luminescence at the wavelengths corresponding to transitions of the BACs in the SBi and GSBi fibres: we observed transitions corresponding to only Si-BACs in the SBi fibres and transitions corresponding to both Si-BACs and Ge-BACs in the GSBi fibres.

Figure 2 illustrates the temperature effect on the optical loss spectra of the bismuth-doped silica, SBi-H and SBi-P fibres in the range 380–850 nm. Note that the holes in the SBi-H fibre were filled with air at room temperature and then heat-sealed hermetically.

In the spectrum of the SBi-H fibre (Fig. 2a), the strength of the absorption bands decreases significantly starting at 700 °C throughout the range 400–850 nm, in particular at 420 and 820 nm ($SE_0 \rightarrow SE_3$ and $SE_0 \rightarrow SE_2$, transitions, see Fig. 1b). After cooling from 1200 °C to RT at a rate of 10 °C min^{-1}, the absorption in this fibre was under 10 dB m^{-1} over the entire spectral range studied.

The variation of the absorption spectrum of the SBi-P fibre on heating (Fig. 2b) differs markedly from that for the SBi-H fibre: there is no sharp drop in absorption above 700 °C in the spectral range studied. The inset in Fig. 1b shows the variation in the absorption at 420 and 820 nm. Also shown for comparison is the variation in the absorption at 650 nm (between the above bands). In the temperature range 30–600 °C, the absorption in the spectral range under consideration varies only gradually. The most marked drop in absorption (by about a factor of 1.4) occurs at 420 nm. We observe a gradual increase in optical loss in the range 600–1000 °C and a steep rise starting at 1000 °C, with a maximum in absorption at ~1130 °C and a drop at higher temperatures. After cooling of the fibre from 1200 °C to RT at a rate of 10 °C min^{-1} [Fig. 2b, curve RT(1)], the optical loss considerably exceeded its original level [Fig. 2b, curve RT(0)] over the entire spectral range examined.

Figure 3 illustrates the temperature effect on the luminescence spectra of the fibres at excitation wavelengths of 457 and 808 nm. The spectra show, in addition to BAC luminescence peaks, luminescence bands at 600 nm, corresponding to Bi^{2+} luminescence [7], and narrow, strong peaks near 800 and 915 nm, which correspond to the scattered pump radiation of the neodymium laser and its first harmonic. In the temperature range 30 to 1000 °C, the 600-nm luminescence intensity in the SBi-H fibre decreased starting at 200 °C and dropped to zero (to the detection limit) at a temperature near 400 °C. The 830-nm luminescence intensity ($SE_2 \rightarrow SE_0$ transition, see Fig. 1b) gradually decreased starting at 300 °C and reached the detection limit near 800 °C. The 1400-nm luminescence intensity ($SE_1 \rightarrow SE_0$ transition) first increased, reaching a maximum near 400 °C, and then gradually decreased to ~740 °C and dropped sharply to the detection limit at higher temperatures. The observed increase in 1400-nm emission intensity at temperatures above 820 °C is due to the increase in thermal radiation level (see below). After cooling from 1000 °C to RT at a rate of 10 °C min^{-1}, no luminescence was detected in the SBi-H fibre.

Figure 3c shows the luminescence spectra of the SBi-H fibre under excitation at 808 nm at temperatures from 30 to 1000 °C. The luminescence spectrum consists of two broad bands centred at 830 and 1400 nm, in agreement with earlier results [7, 12]. The 830-nm luminescence intensity gradually decreased as the temperature was raised from 30 to 800 °C, whereas the 1400-nm luminescence intensity first increased, reaching a maximum near 500 °C, and gradually decreased at higher temperatures. After cooling from 1000 °C to room

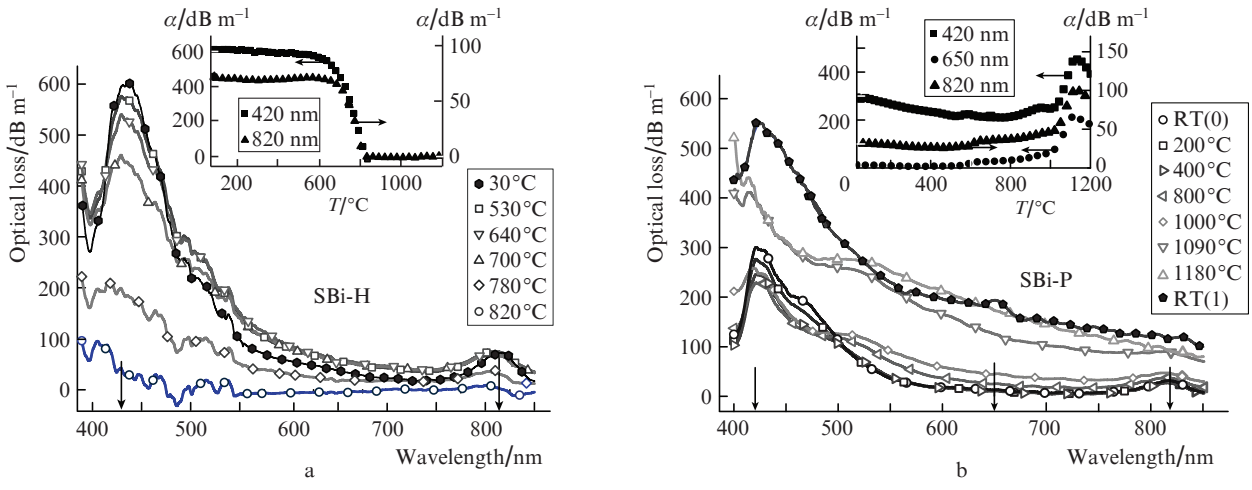

Figure 2. Optical loss spectra of the (a) SBi-H and (b) SBi-P fibres at temperatures from 30 to 1200 °C. Insets: optical loss α as a function of temperature T for the absorption bands at the specified wavelengths.

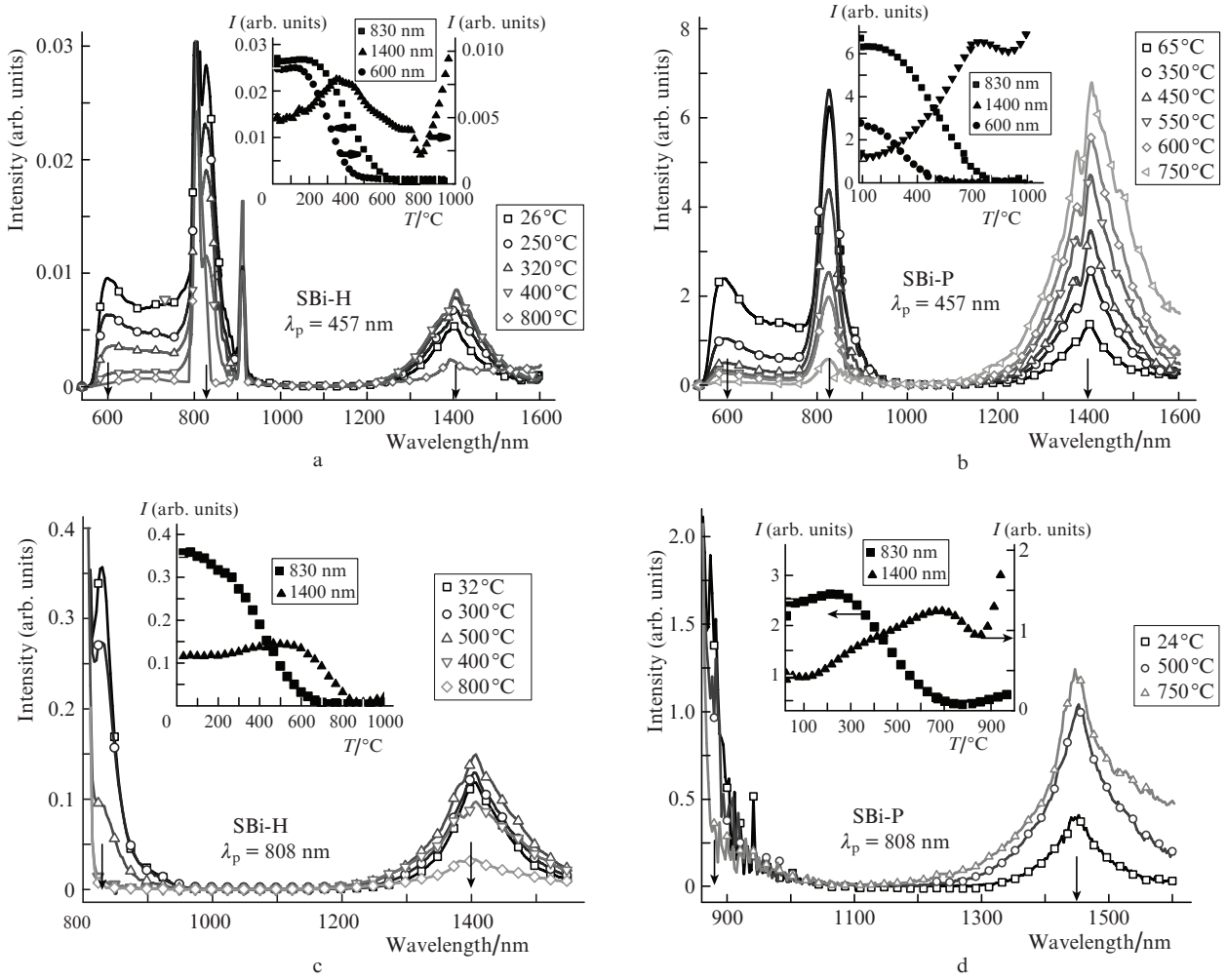

Figure 3. Luminescence spectra of the bismuth-doped fibres (a, c) SBi-H and (b, d) SBi-P in air at excitation wavelengths $\lambda_p =$ 457 and 808 nm and temperatures from 30 to 1000 °C.

temperature at a rate of 10 °C min^{-1}, no luminescence was detected in the SBi-H fibre at this excitation wavelength either.

Figures 3b and 3d show analogous dependences of luminescence spectra for the SBi-P fibre. At an excitation wavelength of 457 nm (Fig. 3b), the 600-nm luminescence intensity also decreased (starting at 200 °C) and reached the detection limit near 400 °C. The 830-nm luminescence intensity gradually decreased with increasing temperature, reaching the detection limit near 800 °C. The 1400-nm luminescence intensity first increased significantly, reaching a maximum at ~750 °C, and then decreased only gradually, with no sharp drop to the detection limit, in contrast to the case of the SBi-H fibre.

After cooling from 1200 °C to RT, the luminescence spectrum of the SBi-P fibre was essentially identical to that before heating, except for the decrease in the intensity of the 600-nm luminescence band compared to the 830-nm band.

As shown above, 700 °C is a threshold temperature at which the 420-nm absorption in the SBi-H fibre decreases considerably. In addition, near 700 °C the 1400-nm luminescence intensity under excitation at 457 nm drops sharply. This agrees with earlier results [7], which demonstrate that the Si-BAC is responsible for both the 420-nm absorption and 1400-nm luminescence.

Figure 3d shows luminescence spectra of the SBi-P fibre at an excitation wavelength of 808 nm. The luminescence spectra consist of two broad bands centred at 830 and 1400 nm. Their intensities vary with temperature in almost the same manner as under excitation at 457 nm. The increase in the 1400-nm luminescence intensity near 1000 °C is due to the rise in thermal radiation intensity.

Analogous data for the GSBi fibre are presented in Fig. 4. We observed not only the Si-BAC and Bi^{2+} luminescence bands at 600 nm (like in the SBi-H and SBi-P fibres) but also the 950-nm luminescence band of the Ge-BAC. The behaviour of the Si-BAC luminescence bands in this fibre is similar to that in the SBi-P. The most drastic distinction from the other fibres studied is the negative slope of the temperature dependence of the 600-nm Bi^{2+} luminescence intensity even at RT. Moreover, the 1400-nm luminescence intensity has a maximum at 450 °C (in contrast to the 750 °C peak in the SBi-P fibre).

Figure 5a illustrates the temperature effect on the optical loss in the GSBi fibre in the spectral range 400–850 nm. Both the absolute change in the optical absorption in the Si-BAC (420 and 820 nm) and Ge-BAC (460 nm) bands and the relationship between neighbouring lines, namely in the 420/460 nm pair, are of interest. Starting at ~700 °C, the absorption at 460 nm rises more rapidly than that at 420 nm.

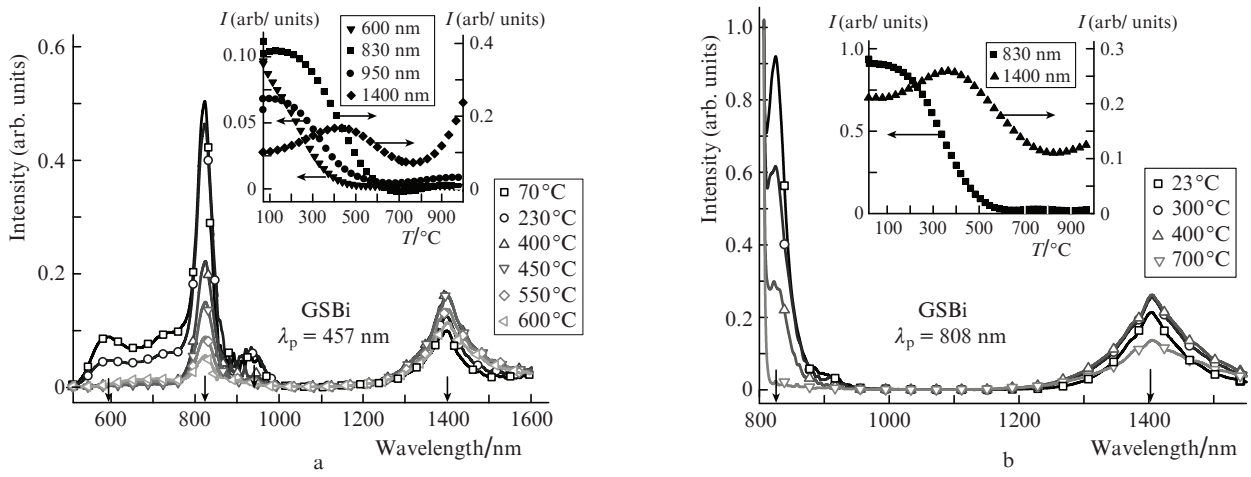

Figure 4. Luminescence spectra of the GSBi fibre in air at excitation wavelengths λ_p = (a) 457 and (b) 808 nm and temperatures from 30 to 1000 °C.

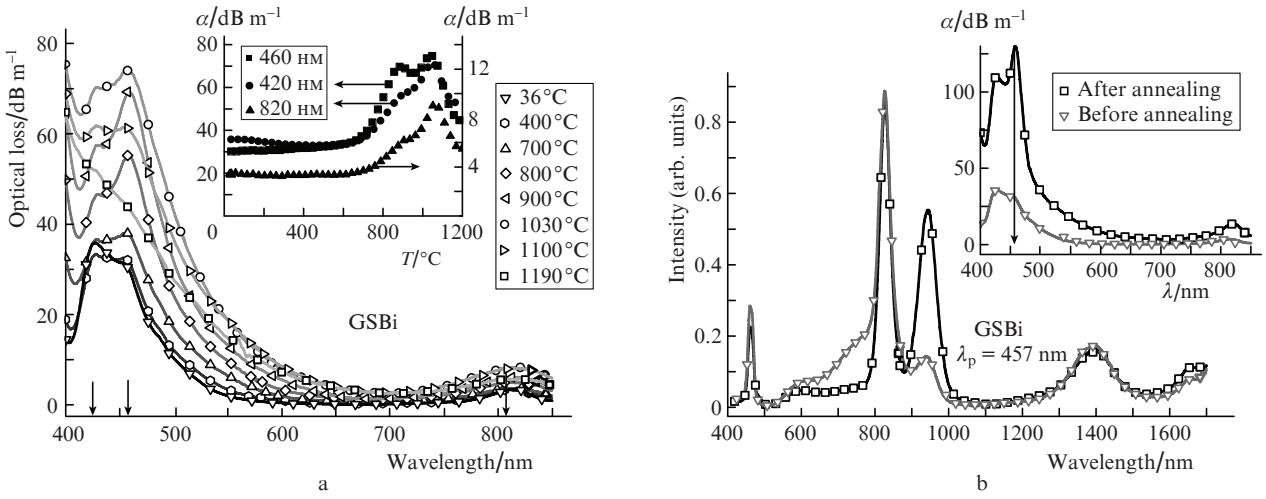

Figure 5. (a) Optical loss (α) spectra of the GSBi fibre at different temperatures. Inset: α vs. T at the specified wavelengths. (b) Luminescence spectra of the GSBi fibre before and after annealing at 1000 °C (λ_p = 457 nm). Inset: optical loss spectra of the fibre before and after annealing.

At higher temperatures, the 460-nm band has two local maxima in absorption coefficient, at 830 and 1030 °C. Above 1030 °C, the absorption decreases in all the above lines. The temperature dependences of absorption for the Si-BAC lines have only one maximum, near 1030 °C (in contrast to that for the 460-nm Ge-BAC line).

Figure 5b shows the room-temperature luminescence spectra of the GSBi fibre before and after heating to 1000 °C and subsequent cooling. The inset in Fig. 5b presents the loss spectra of this fibre before and after the heating/cooling cycle. Comparison of the spectra indicates a marked increase in 460-nm absorption relative to the 420-nm absorption band. At the same time, we observe an increase in luminescence intensity near 950 nm at an excitation wavelength of 457 nm.

Comparison of the data in Figs 5a and 5b demonstrates that heating increases the concentrations of Si-BACs (~420-nm absorption) and Ge-BACs (~460-nm absorption) [7] in the GSBi fibre. In addition, the Ge-BAC luminescence and absorption increase by several times relative to the Si-BACs.

4. Discussion

Up to ~700 °C, heating of the fibres studied here causes no significant changes in their absorption coefficient in the BAC lines. At the same time, we observe marked changes in luminescence intensity for various transitions of the BACs. In particular, in all the fibres the 1400-nm luminescence intensity increases, whereas the 830-nm luminescence intensity drops (Figs 3, 4). Similar results were obtained by Bazakutsa et al. [15] in the range 20–600 °C for silica glass doped with bismuth by the SPCVD process. To understand this effect, we investigated the 1400-nm luminescence kinetics in the GSBi fibre at an excitation wavelength of 808 nm and different temperatures (Fig. 6). After a 10-μs excitation pulse, we observed a luminescence rise with a temperature-dependent, short characteristic time (25 μs or shorter), followed by a luminescence decay with a characteristic time of ~600 μs. The luminescence rise time, which characterises the Si-BAC lifetime at the SE_2 level (Fig. 1b), corresponding to the 820-nm absorption and 830-nm luminescence, decreases sharply with increasing temperature, down to 3 μs near 800 °C. This accounts for the reduction in 830-nm luminescence intensity and the

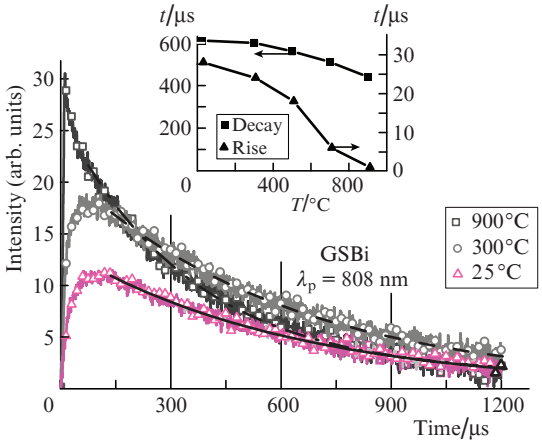

Figure 6. Luminescence intensity as a function of time t for the GSBi fibre under excitation with 10-μs pulses at 808 nm. Inset: temperature dependences of the 1400-nm luminescence rise and decay times at an excitation wavelength $\lambda_p = 808$ nm.

accompanying increase in 1400-nm luminescence intensity on heating: with increasing temperature, the probability of non-radiative decay from the SE_2 level to the SE_1 increases.

Our measurements showed that heating to 800 °C reduced the optical absorption and luminescence at the wavelengths of the Si-BAC in the SBi-H fibre, containing air-filled holes ~1 μm from its about 6-μm-diameter core, to almost zero (Figs 2a, 3a, 3c), which indicates that no BACs persisted in the fibre core. In the fibre containing no air-filled holes (SBi-P), BACs persisted under similar conditions (Figs 2b, 3b, 3d). Note that a similar effect was found earlier to occur during SBi-H fibre drawing in an oxygen atmosphere [13]; drawing itself occurs near 2000 °C. In our experiments, BACs disappeared at a substantially lower temperature, near 800 °C.

The SBi-H and SBi-P fibres differ in that the distance from their core to the interface with oxygen gas is ~1 μm in the former and near 60 μm in the latter. It is therefore reasonable to assume that oxygen diffusion in the SBi-H fibre at elevated temperatures leads to BAC dissociation. However, according to Williams [16] the diffusion distance of oxygen in v-SiO_2 at 800 °C over a period of ~15 min, characteristic of our experiments, is no greater than 0.03 μm. At the same time, in our experiments diffusion occurred in a fibre material whose glass structure differed from that of conventional v-SiO_2 by a larger percentage of distorted bonds and lower density because it resulted from rapid cooling during fibre drawing [17]. The diffusion coefficient in such materials may considerably exceed that in glass obtained by slow cooling (see e.g. Ref. [18]).

Thus, tentatively assuming that each of the BACs comprises a bismuth ion and a glass network defect [6], we infer from the present results that the bismuth in the BACs should have a low valence (and further oxidation of the bismuth causes the centres to disappear) and the glass network defect in question is oxygen-deficient.

The distribution of oxygen-deficient centres in the core of germanosilicate fibres is known to be nonuniform, with a maximum at the interface with the reflective cladding [19]. In view of this, we performed additional measurements of the 830-nm luminescence distribution under 457-nm excitation and the 230-nm absorption distribution across the SBi-P fibre preform.

It is also known that bismuth-doped glasses have a UV absorption band whose position, usually 200–300 nm, depends on glass composition [20]. It seems commonly accepted that this band is due to Bi^{3+} (see e.g. Refs [20, 21]). The inset in Fig. 7 shows the absorption spectrum of the SBi-P fibre preform core and, for comparison, that of a similar preform having a bismuth-free core (spatial resolution, ~0.1 mm). Clearly, the absorption band centred at 230 nm is due to Bi doping and, according to the above, arises from Bi^{3+}. Therefore, the radial profile of the 230-nm absorption coefficient represents the Bi^{3+} distribution across the preform core. At the same time, the 830-nm luminescence brightness profile should provide information (under uniform excitation) about the Si-BAC distribution.

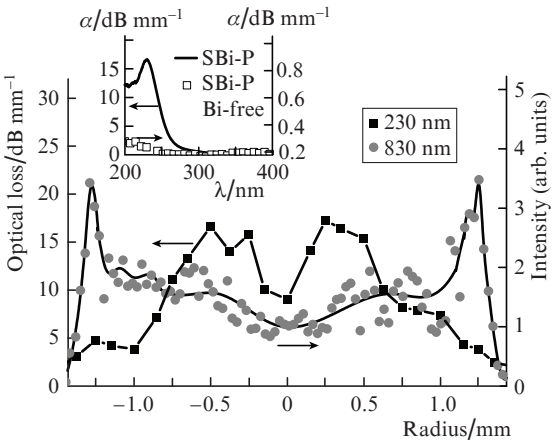

Figure 7. Radial profiles of the 230-nm optical loss α and 830-nm luminescence intensity in the SBi-P fibre preform. Inset: optical loss spectra of the SBi-P fibre preform core and a similar, bismuth-free preform.

The profiles in Fig. 7 differ markedly from one another. Whereas the Bi^{3+} concentration has a maximum in the middle part of the core (with a central dip), the Si-BAC concentration (830-nm luminescence intensity) peaks near the core–cladding interface, with an increased Si-BAC concentration in a region located about 0.4 mm from the interface. Thus, the BAC distribution across the preform differs significantly from the Bi^{3+} distribution and has a maximum near the interface with the reflective cladding, in qualitative agreement with the oxygen-deficient centre distribution in germanosilicate preforms [19]. This suggests that oxygen-deficient centres in the glass may be involved in the formation of IR-emitting bismuth centres.

Significant temperature quenching of the 600-nm luminescence occurs even at 400 °C (Figs 3, 4). However, the distinctions between the temperature dependences of the 600- and 830-nm luminescence intensities both during the experiment (SBi-P, SBi-H and GSBi fibres) and after heat treatment at 1200 °C followed by slow cooling (SBi-P fibre) indicate that these bands are due to different active centres [7].

We call attention to the temperature dependences of the 1400-nm luminescence intensity for the three fibres at an excitation wavelength of 457 nm (Fig. 8). The inset in Fig. 8 shows the optical loss as a function of temperature for the 420- and 460-nm absorption bands of the GSBi fibre. The presence of air near the core of the SBi-H fibre reduces the 1400-nm luminescence intensity (Si-BAC) at temperatures above 400 °C.

The absence of excess oxygen near the core of the SBi-P fibre reduces the 1400-nm luminescence intensity only above ~750 °C. At the same time, the curve of the GSBi fibre is similar in shape to that of the SBi-H holey fibre, even though the GSBi fibre has no holes. The absorption spectrum of the GSBi fibre suggests that the concentration of Si-BACs, responsible for the 420-nm absorption band, decreased as the temperature was raised to ~700 °C, whereas the concentration of Ge-BACs, responsible for the 460-nm absorption band, increased. Thus, it is reasonable to assume that the GeO_2 in the GSBi fibre acts as an oxygen source for the Si-BACs, like the air in the holes of the SBi-P fibre. In the GSBi fibre, however, the transformation of the Bi-related active centres is a reversible process: after cooling, the IR-emitting centres in this fibre persist (Fig. 5b), and the Ge-BAC concentration increases by several times relative to the Si-BACs. We think that such temperature behaviour of the Si-BAC and Ge-BAC centres also supports the model in which each of the Bi-related active centres comprises a bismuth ion and an oxygen-deficient glass network defect [6].

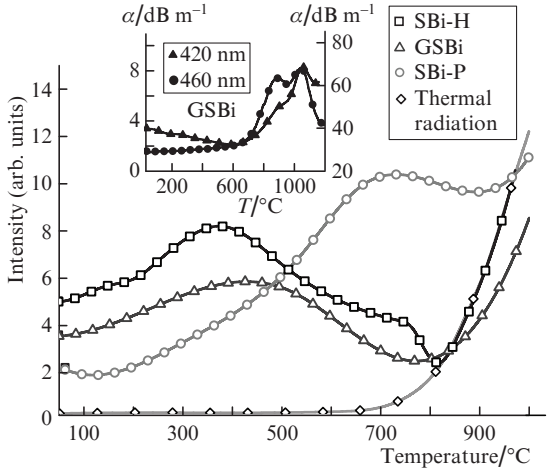

Figure 8. Temperature dependences of the 1400-nm luminescence intensity for the SBi-H, SBi-P and GSBi fibres at an excitation wavelength of 457 nm and that of the thermal radiation intensity for the SBi-H fibre. Inset: optical loss α as a function of temperature T for the 420- and 460-nm absorption bands of the GSBi fibre.

As an illustration, Fig. 8 shows the temperature dependence of the 1400-nm thermal radiation intensity measured under the same conditions as the 1400-nm luminescence intensity in the SBi-H fibre but with the excitation source turned off. Comparison of the two curves indicates that, at temperatures above 800 °C, the thermal radiation intensity considerably exceeds the luminescence intensity. In the other fibres (especially at shorter wavelengths), the relative contribution of thermal radiation is markedly smaller, but it was observed in all luminescence measurements. It is worth noting here that the SBi-H fibre had the lowest luminescence intensity among the three fibres, which increased the relative contribution of the thermal radiation.

Attention should also be paid to the sharp increase in absorption at high temperatures in the spectral range under consideration – starting at T = 1030 °C in the SBi-P fibre (Fig. 2b) and at T = 700 °C in the GSBi fibre (Fig. 5a) – and the decrease in optical loss at temperatures above 1130 °C in the SBi-P fibre and starting at 1030 °C in the GSBi. Further research is needed to shed light on this effect.

5. Conclusions

The absorption and luminescence bands of bismuth-doped silica and germanosilicate fibres have been measured for the first time as a function of temperature. Heating of a bismuth-doped holey silica fibre in the presence of oxygen between 700 and 800 °C was found to markedly reduce the absorption and luminescence bands of bismuth-related active centres. Without oxygen, no such effect was detected. This finding, in conjunction with earlier results [13], suggests that the BACs studied contain low-valence bismuth ions associated with oxygen-deficient glass network defects.

The Si-BAC lifetime at the SE_2 level was found to decrease sharply (from 30 to less than 3 μs) on heating from room temperature to 900 °C (Fig. 1b), whereas the 1400-nm luminescence lifetime ($SE_1 \rightarrow SE_0$ transition) decreases by 25% in this temperature range.

Heating the bismuth-doped germanosilicate fibre increases the absorption in all the bands of the bismuth-related active centres (both the Si-BACs and Ge-BACs). The absorption and luminescence in the Ge-BACs increase by several times relative to the Si-BACs.

The Bi^{3+} profile across the preforms differs markedly from the Si-BACs profile. The Si-BAC concentration in the silica fibre has a maximum near the core–cladding interface (like the oxygen-deficient centre concentration in the germanosilicate fibres), which provides additional evidence that the BACs may be associated with oxygen-deficient structural defects of the glass.

Acknowledgements. This work was supported in part by the Russian Foundation for Basic Research (Grant No. 11-02-01318) and the Presidium of the Russian Academy of Sciences (basic research programme No. 22).

References

1. Bufetov I.A., Dianov E.M. *Laser Phys. Lett*., **6**, 487 (2009).
2. Firstov S.V., Shubin A.V., Khopin V.F., Mel'kumov M.A., Bufetov I.A., Medvedkov O.I., Gur'yanov A.N., Dianov E.M. *Kvantovaya Elektron*., **41**, 581 (2011) [*Quantum Electron*., **41**, 581 (2011)].
3. Melkumov M.A., Bufetov I.A., Shubin A.V., Firstov S.V., Khopin V.F., Guryanov A.N., Dianov E.M. *Opt. Lett*., **36**, 2408 (2011).
4. Dianov E.M., Krylov A.A., Dvoyrin V.V., Mashinsky V.M., Kryukov P.G. *J. Opt. Soc. Am. B*, **24**, 1807 (2007).
5. Peng M., Dong G., Wondraczek L., Zhang L., Zhang N., Qiu J. *J. Non-Cryst. Solids*, **357**, 2241 (2011).
6. Dianov E.M. *Kvantovaya Elektron*., **40** (4), 283 (2010) [*Quantum Electron*., **40** (4), 283 (2010)].
7. Firstov S.V., Khopin V.F., Bufetov I.A., Firstova E.G., Guryanov A.N., Dianov E.M. *Opt. Express*, **19**, 19551 (2011).
8. Bulatov L.I., Mashinsky V.M., Dvoyrin V.V., Kustov E.F., Dianov E.M., Sukhorukov A.P. *Izv. Akad. Nauk, Ser. Fiz*., **72**, 1751 (2008).
9. Kashyap P. *Proc. Intern. Conf. Lasers'87* (Lake Tahoe, Nevada, 1987) p. 859.
10. Hand D.P., Russell P.St.J. *Opt. Lett*., **13**, 767 (1988).
11. Davis D.D., Meller S.C., DiGiovanni D.J. *Proc. SPIE Int. Soc. Opt. Eng*., **2966**, 592 (1997).
12. Bufetov I.A.,Melkumov M.A., Firstov S.V., Shubin A.V., Semenov S.L., Vel'miskin V.V., Levchenko A.E., Firstova E.G., Dianov E.M. *Opt. Lett*., **36**, 166 (2011).

13. Zlenko A.S., Dvoyrin V.V., Mashinsky V.M., et al. *Opt. Lett.*, **36**, 2599 (2011).
14. Mattsson K.E. *Opt. Express*, **19**, 19797 (2011).
15. Bazakutsa A.P., Butov O.V., Golant K.M. *Mater. III Vseross. konf. po volokonnoi optike* (Proc. III All-Russia Conf. on Fibre Optics) (Perm, 2011) No. 6, p. 108.
16. Williams E.L. *J. Am. Ceram. Soc*., **48**, 190 (1965).
17. Vogel W. *Glass Chemistry* (Berlin–Heidelberg: Springer-Verlag, 1994).
18. Mehrer H. *Diffusion in Solids* (Berlin–Heidelberg: Springer-Verlag, 2007).
19. Neustruev V.B. *J. Phys.: Condens. Matter*, **6**, 6901 (1994).
20. Duffy J.A., Ingram M.D. *J. Chem. Phys*., **52** (7), 3752 (1970).
21. Denker B.I., Galagan B.I., Shulman I.I., Sverchkov S.E., Dianov E.M. *Appl. Phys. B*, **103**, 681 (2011).